Nonisotropic effective-medium approximation for diffusion problems in random media

Eduardo R. Reyes
Departamento de Física, Universidad Nacional del Comahue, 8300 Neuquén, Argentina

Manuel O. Cáceres*
Centro Atómico Bariloche and Instituto Balseiro, Comisión Nacional de Energía Atómica and Universidad Nacional de Cuyo, 8400 San Carlos de Bariloche, Río Negro, Argentina

Pedro A. Pury
Facultad de Matemática, Astronomía y Física, Universidad Nacional de Córdoba, Ciudad Universitaria, 5000 Córdoba, Argentina
(Received 22 March 1999; revised manuscript received 7 July 1999)

We present the nonisotropic effective-medium approximation to solve diffusion problems in a two-dimensional anisotropic random media. The problem has been worked out by introducing a generalization of the well-known effective-medium approximation. A set of coupled nonlinear self-consistent equations must be solved to find the effective rates in each direction. We have considered (analytically) some particular models in short and large frequency limits. The dc conductivity is also compared against the isotropic case. The ac conductivity and Cole-Cole diagrams for the nonisotropic random bond percolation model have been analyzed in terms of the physical parameters that characterize the anisotropy and the disorder in the media. A mono-parametric nonisotropic bond disordered model (α model) has also been worked out to show the applicability of the present approach in the context of weak or strong disorder. Such a model of disorder leads the system to show a quasi-one-dimensional behavior, proper of nonisotropic materials.

I. INTRODUCTION

We are interested in the study of anomalous *pure*-diffusion (i.e., without bias) and ac-electric conductivity on nonisotropic random media. Typical examples where the frequency-dependent response needs to be found belong to the field of solid-state transport, but also in geological studies[1] (dielectric properties of reservoir rocks) the transport on anisotropic heterogeneous media needs to be characterized.[2] Let us mention here that ac conductivity measurements of $La_2NiO_{4+\delta}$ have recently been carried out[4] showing a strong anisotropy in the electric conductivity. The characteristics of these materials can be summarized as follows: (i) the system has strong nonisotropic three-dimensional (3D) behavior (which has been established through dc measurements) suggesting that the conductivity in the NiO_2 basal plane exceeds the one along the orthogonal *c* axis by two orders of magnitude; (ii) the frequency behavior of the $\mathrm{Re}[\sigma(2\pi f)]$ shows a power law $(2\pi f)^s$ for intermediate frequencies, with an exponent in the range $0.38 < s < 0.8$; (iii) this system involves weak Anderson localized states, therefore justifying the use of a hopping stochastic model for its transport description. Here we propose a general description of anisotropic anomalous diffusion within a stochastic transport theory that allows the interplay of anisotropy and disorder.

The stochastic transport theory has been developed independently by Scher and Lax[5] and Alexander *et al.*[6] In particular, Odagaki and Lax[7] have employed the effective-medium approximation (EMA) to calculate the averaged random walk propagator, obtaining in this way a generalized Einstein relation from a mesoscopic point of view. It is known that EMA gives the correct anomalous diffusion exponent for unbiased walks,[6,8] but also more complex systems such as conductivity in granular metal film[9] can be described in the context of EMA. In the recent past, several extensions of EMA have been performed to study the first passage time distribution in finite chains,[10,11] and the injection of external current of particles in random media.[12,13]

In the present work, we extend the EMA considering a 2D disordered system that also presents anisotropy. For this purpose we introduce different bond disorder distributions for each direction in the lattice (namely horizontal and vertical). Thus a set of coupled nonlinear self-consistent equations must be solved to find effective diffusion constants in each direction. We calculate the nonisotropic ac conductivity for the bond percolation model, and the dc conductivity for another class of disorder presenting weak and strong limits. As a matter of fact, the nonisotropic dc conductivity for bond percolation was previously reported by using Kirkpatrik's approach for square and cubic lattices,[14] and for triangular lattices,[15] too. In Bernasconi's paper the author considers an effective electric network, and analyzes the perturbation produced on the voltage across the resistances by changing a single conductance oriented along each direction of the external electric field. Thus the effective conductivities are determined by the requirement that the voltage variations should average zero. In a previous paper, using our generalized EMA we have studied the dc conductivity on a 2D nonisotropic percolation network.[16] Here, we extend these studies to consider the spectral behavior and other models of disorder, too. For simplicity, we restrict the problem for square lattice, but it can also be extended to 3D.

We start our description with a 2D random walk (RW) on a random nonisotropic media, which can be represented by a one-step master equation with discrete indexes.[17] In Sec. II

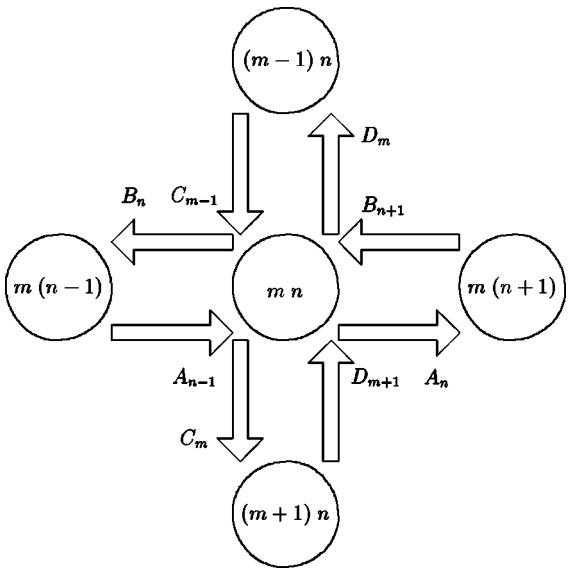

FIG. 1. Definitions of hopping rates associated with the site (m,n) for the general case in the square lattice. The circles represent sites in the lattice.

the general theory of nonisotropic EMA is presented, all the calculations have been done on square lattices. Section III is devoted to present some cases of anisotropic percolation, and weak and strong disorder models. In Sec. IV we present the conclusions concerning our approach. The mathematical details concerning Green's functions and the density of states in anisotropic lattices can be found in the Appendixes.

II. 2D NONISOTROPIC EMA

A. Nonisotropic ordered case

For a random walk (RW) on a d-dimensional lattice, the dynamics of the particle is governed by the master equation

$$\frac{\partial}{\partial t}P(\vec{s},t|\vec{s}_0,0)=-\Gamma_{\vec{s}}P(\vec{s},t|\vec{s}_0,0)+\sum_{\vec{s}'(\neq\vec{s})}W_{\vec{s},\vec{s}'}P(\vec{s}',t|\vec{s}_0,0), \tag{2.1}$$

where $\vec{s}$ represents an arbitrary d-dimensional vector on the lattice, $W_{\vec{s},\vec{s}'}$ is the hopping probability transition from site $\vec{s}'$ to site $\vec{s}$, $\Gamma_{\vec{s}}=\Sigma_{\vec{s}'(\neq\vec{s})}W_{\vec{s}',\vec{s}}$ is the escape rate from the site $\vec{s}$, and $P(\vec{s},t|\vec{s}_0,0)$ is the conditional probability of finding the particle at site $\vec{s}$ at time t, given that it initially was at site $\vec{s}_0$. Introducing the RW operator

$$H=-\sum_{\vec{s}}|\vec{s}\rangle\Gamma_{\vec{s}}\langle\vec{s}|+\sum_{\vec{s}',(\neq\vec{s})}|\vec{s}\rangle W_{\vec{s},\vec{s}'}\langle\vec{s}'|, \tag{2.2}$$

the formal solution of Eq. (2.1) in the Laplace representation (i.e., $t\rightarrow u$) results in

$$\hat{P}(\vec{s},u|\vec{s}_0)=\langle\vec{s}|(u-H)^{-1}|\vec{s}_0\rangle\equiv G_{\vec{s},\vec{s}_0}(u), \tag{2.3}$$

where $G(u)$ denotes the Green's function or propagator of the RW operator H. In the square lattice and for transition only to nearest-neighbor sites, Eq. (2.1) reads

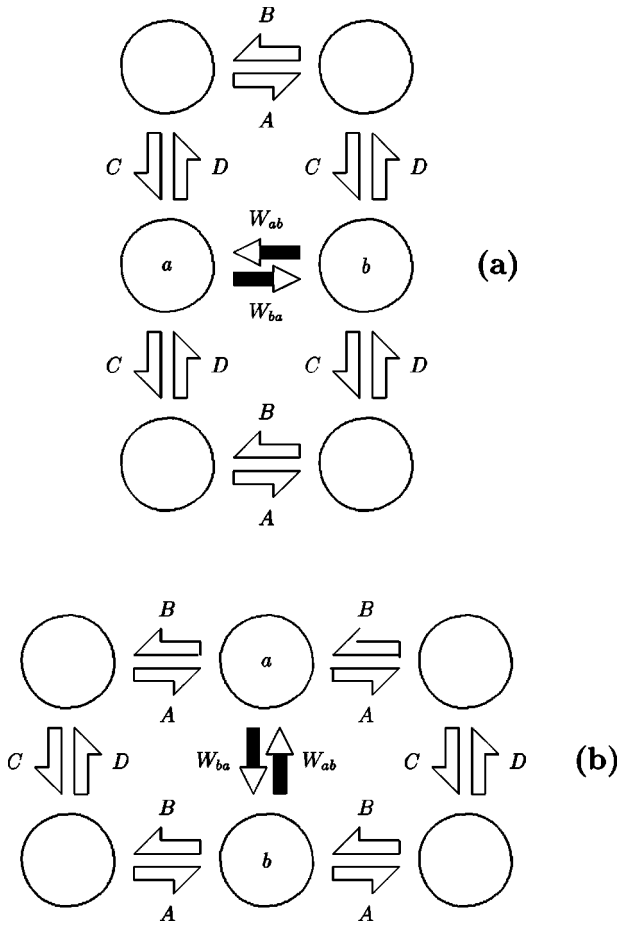

FIG. 2. Sketch of the single impurity problem. A substitutional impurity has been allocated between the nearest-neighbor sites a and b in the square lattice. The pair of sites a, b can be set in the horizontal direction (a) or in the vertical direction (b).

$$\begin{aligned}\partial_t P_{m,n}(t)=&A_{n-1}P_{m,n-1}(t)+B_{n+1}P_{m,n+1}(t)\\&+C_{m-1}P_{m-1,n}(t)+D_{m+1}P_{m+1,n}(t)\\&-(A_n+B_n+C_m+D_m)P_{m,n}(t),\end{aligned} \tag{2.4}$$

where $P_{m,n}(t)$ is the conditional probability of finding the particle at site (m,n) and time t given the initial condition $P_{m,n}(0)=\delta_{m,m_0}\delta_{n,n_0}$. The hopping rates are defined in Fig. 1. The general nonrandom (ordered) case in the square lattice corresponds to site-independent transition rates. The associated RW operator results

$$\begin{aligned}H_0=&A|m,n\rangle\langle m,n-1|+B|m,n\rangle\langle m,n+1|\\&+C|m,n\rangle\langle m-1,n|+D|m,n\rangle\langle m+1,n|\\&-(A+B+C+D)|m,n\rangle\langle m,n|.\end{aligned} \tag{2.5}$$

A complete treatment for the solution of the biased nonisotropic 2D problem can be found in Appendix A.

We now consider the *single impurity* problem in which the homogeneity of the ordered lattice has been destroyed at just one bond (the bond that connects the nearest-neighbor sites a and b on the square lattice). There the transition rates equal W_{ab} and W_{ba}; at every other bond it has the unperturbed values A,B or C,D, corresponding to horizontal or vertical bonds (see Fig. 2). The RW operator can be written

as $H_i = H_0 + V$, where H_0 is given by Eq. (2.5) and V is the perturbation arising from the substitutional impurity

$$V_{\alpha\beta} = b_1\delta_{\alpha a}\delta_{\beta a} + b_2\delta_{\alpha a}\delta_{\beta b} + b_3\delta_{\alpha b}\delta_{\beta a} + b_4\delta_{\alpha b}\delta_{\beta b}. \tag{2.6}$$

$\delta_{\alpha\beta}$ is the Kronecker delta. We have defined $b_1 = A - W_{ba}$, $b_2 = W_{ab} - B$, $b_3 = W_{ba} - A$, and $b_4 = B - W_{ab}$ if the sites a and b are horizontal nearest-neighbor sites [see Fig. 2(a)] and $b_1 = C - W_{ba}$, $b_2 = W_{ab} - D$, $b_3 = W_{ba} - C$, and $b_4 = D - W_{ab}$ if the sites a and b are vertical nearest-neighbor sites [see Fig. 2(b)]. The Green's function corresponding to the single impurity problem, $G^i(u) = (u - H_i)^{-1}$, can be expressed in terms of Green's function associated to the ordered lattice, $G^0(u) = (u - H_0)^{-1}$, as is shown in Eq. (B6) (Appendix B).

B. Nonisotropic random case

In the square lattice, the general random case corresponds to the situation for which hopping rates A_n, B_n, C_m, D_m in Eq. (2.4) are independent, identically distributed random variables. Thus the general case involves four distributions. For the nonisotropic unbiased case we take $A_n = B_{n-1}$ and $C_m = D_{m+1}$. Thus the disorder is now characterized by two distributions of transitions rates, corresponding to the horizontal and vertical directions. Here EMA consists in calculating the average effects of disorder by defining a coherent medium with two effective rates (u dependent). These effective rates are self-consistently determined by the requirement that the difference between the propagator of the impurity and homogeneous problem should average zero. Thus in nonisotropic unbiased problems, for each direction, horizontal and vertical, we introduce unknown effective rates, $w^{\leftrightarrow}_{\rm eff}(u)$ and $w^{\updownarrow}_{\rm eff}(u)$, which are determined by (two) self-consistent conditions:

$$\langle G^i_{ab}(u, w^{\leftrightarrow}_{\rm eff}, w^{\updownarrow}_{\rm eff}, w^{\leftrightarrow})\rangle_{\Gamma(w^{\leftrightarrow})} = G^0_{ab}(u, w^{\leftrightarrow}_{\rm eff}, w^{\updownarrow}_{\rm eff}),$$

$$\langle G^i_{ab}(u, w^{\leftrightarrow}_{\rm eff}, w^{\updownarrow}_{\rm eff}, w^{\updownarrow})\rangle_{\Omega(w^{\updownarrow})} = G^0_{ab}(u, w^{\leftrightarrow}_{\rm eff}, w^{\updownarrow}_{\rm eff}). \tag{2.7}$$

$G^i_{a,b}$ and $G^0_{a,b}$ are the *single impurity* and the *nonperturbed* nonisotropic Green's functions, respectively. The impure bond connects the nearest-neighbor sites a and b. The transition rates between these sites are equal to $w^{\leftrightarrow}$ if the bond lies in the horizontal direction and $w^{\updownarrow}$ if the impure bond is vertical. $\Gamma(w^{\leftrightarrow})$ and $\Omega(w^{\updownarrow})$ are the probability distributions assigned to the random variables $w^{\leftrightarrow}$ and $w^{\updownarrow}$, respectively. These distributions describe the model of nonisotropic unbiased disorder in the lattice. Note that considering a perturbed Green's function with two impure bonds (namely one in the vertical and one in the horizontal axis) would correspond to considering higher-order Terwiel's cumulants that are beyond EMA.[8,12] Considering the explicit form of the Green's functions involved in Eq. (2.7) (see the Appendixes with the substitutions $A = w^{\leftrightarrow}_{\rm eff}$ and $D = w^{\updownarrow}_{\rm eff}$), we can write

$$G^i_{(1,0),(0,0)} = \frac{G^0_{(1,0),(0,0)} + (w^{\leftrightarrow}_{\rm eff} - w^{\leftrightarrow})[(G^0_{(1,0),(0,0)})^2 - (G^0_{(0,0),(0,0)})^2]}{1 + 2(w^{\leftrightarrow}_{\rm eff} - w^{\leftrightarrow})(G^0_{(1,0),(0,0)} - G^0_{(0,0),(0,0)})},$$

$$G^i_{(0,1),(0,0)} = \frac{G^0_{(0,1),(0,0)} + (w^{\updownarrow}_{\rm eff} - w^{\updownarrow})[(G^0_{(0,1),(0,0)})^2 - (G^0_{(0,0),(0,0)})^2]}{1 + 2(w^{\updownarrow}_{\rm eff} - w^{\updownarrow})(G^0_{(0,1),(0,0)} - G^0_{(0,0),(0,0)})}. \tag{2.8}$$

Putting Eq. (2.8) in Eq. (2.7), the self-consistent conditions read

$$\left\langle \frac{w^{\leftrightarrow}_{\rm eff} - w^{\leftrightarrow}}{1 + 2(w^{\leftrightarrow}_{\rm eff} - w^{\leftrightarrow})(G^0_{(1,0),(0,0)} - G^0_{(0,0),(0,0)})} \right\rangle_{\Gamma(w^{\leftrightarrow})} = 0,$$

$$\left\langle \frac{w^{\updownarrow}_{\rm eff} - w^{\updownarrow}}{1 + 2(w^{\updownarrow}_{\rm eff} - w^{\updownarrow})(G^0_{(0,1),(0,0)} - G^0_{(0,0),(0,0)})} \right\rangle_{\Omega(w^{\updownarrow})} = 0. \tag{2.9}$$

Following the linear response theory[7] the generalized diffusion coefficients $D(u)$, in the anisotropic EMA context, are now given by

$$D^{\leftrightarrow}(u) = \Lambda^2 w^{\leftrightarrow}_{\rm eff}(u), \quad D^{\updownarrow}(u) = \Lambda^2 w^{\updownarrow}_{\rm eff}(u), \tag{2.10}$$

where Λ is the lattice constant (we will take $\Lambda = 1$). The stochastic transport theory predicts frequency-dependent conductivity in horizontal [vertical] direction, proportional to the effective rate $w^{\leftrightarrow}_{\rm eff}$ [$w^{\updownarrow}_{\rm eff}$]:

$$\sigma^{\leftrightarrow[\updownarrow]}(\omega) = \frac{ne^2}{kT} D^{\leftrightarrow[\updownarrow]}(u = i2\pi f). \tag{2.11}$$

These are generalized Einstein's relations for nonisotropic random media. Therefore the dielectric constant in each direction can be studied by considering the real and imaginary part of the corresponding Eq. (2.11).

III. NONISOTROPIC DISORDERED MODELS

There are several physical systems where the strong anisotropy leads to the study and the construction of models, where the disorder is only present in one direction. Cases like this can be seen on diffusion-advection stratified media,[18] growth of thin films,[4] etc. In this paper we will consider the case when the disorder is only present in one direction, let us say in the *vertical* direction. Thus we can use our general Eq. (2.9) for the case when $w^{\leftrightarrow}$ is a sure (nonrandom) variable and $w^{\updownarrow}$ is a random one. The general case with two types of disorder (one in each direction) and when there is bias in the system will be reported elsewhere.

A. Bond percolation model

Consider the case where the disordered bonds in the vertical direction are distributed following a random percolation model. Therefore a bond in the vertical direction of the lattice can either be a conducting one with probability p, or insulating with probability $1-p$. The probability measure $\Omega(w^{\updownarrow})$ is given by the dichotomous distribution

$$\Omega(w^{\updownarrow}) = p\,\delta(w^{\updownarrow} - w^{0\updownarrow}) + (1-p)\,\delta(w^{\updownarrow}). \tag{3.1}$$

It is easy to see that even when the fraction $1-p$ of insulating bonds is negligible, the portrait of any realization of dis-

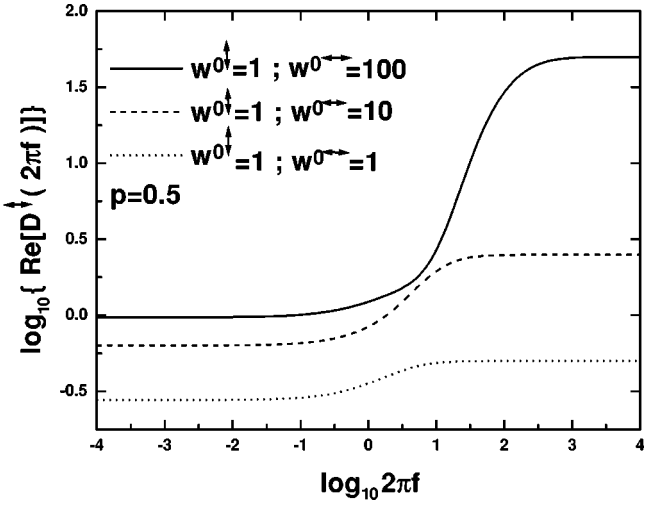

FIG. 3. Log-log plot of the real part of the (nonisotropic) generalized conductivity in the vertical direction as a function of frequency $2\pi f$, for $p=0.5$ and different values of the parameter $w^{0\updownarrow}$ and $w^{0\leftrightarrow}$. At intermediate frequencies the ac conductivity follows an approximate power law $\sigma(2\pi f)\propto(2\pi f)^s$.

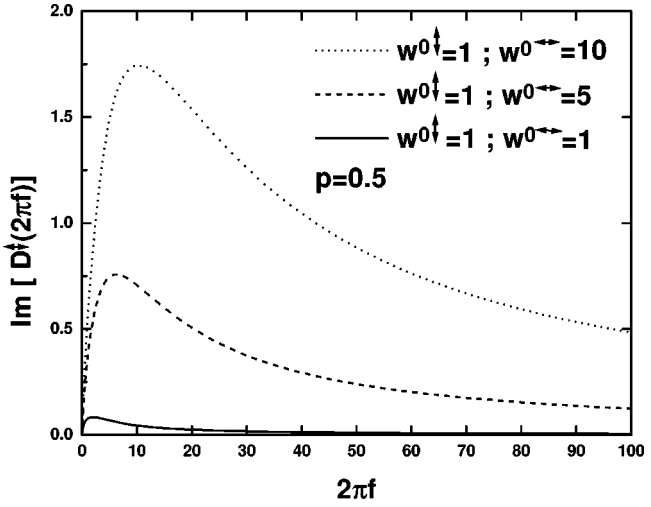

FIG. 4. Frequency behavior of the imaginary part of $D^{\updownarrow}(2\pi f)$, for the same values of the parameters given in Fig. 3. At low frequencies we found a proportionality between $\mathrm{Im}[D^{\updownarrow}(2\pi f)]$ and $2\pi f$.

order will not show the statistical rotational invariance of isotropic models. This simple fact shows that the present model cannot go continuously to the isotropic limit. Because in the present paper $w^{\leftrightarrow}$ is a sure variable, $w^{\leftrightarrow}_{\mathrm{eff}}(u)=w^{0\leftrightarrow}$ (fixed). So from Eq. (2.9) we only get *one* self-consistent equation:

$$pw^{0\updownarrow}-w^{\updownarrow}_{\mathrm{eff}}(u)+2[w^{\updownarrow}_{\mathrm{eff}}(u)w^{0\updownarrow}-(w^{\updownarrow}_{\mathrm{eff}}(u))^2](G^0_{(1,0),(0,0)}(u)-G^0_{(0,0),(0,0)}(u))=0. \tag{3.2}$$

The frequency response is obtained by numerical solution of this self-consistent condition. The corresponding expressions for the Green's functions are given in Appendix A. In Figs. 3 and 4 we show the behavior of the real and imaginary part of the generalized diffusion coefficient in the vertical direction, by introducing the variable change: $u\rightarrow i2\pi f$. In Fig. 3 it is possible to observe that in the low-frequency range the plot is flat and the conductivity is given by its dc value. For the high-frequency region a saturation of $\mathrm{Re}[D^{\updownarrow}(2\pi f)]$ is shown, whereas at intermediate frequencies the ac conductivity follows a power law: $\sigma^{\updownarrow}(2\pi f)\propto(2\pi f)^s$ with $s>0$. This dielectric response has been observed in a broad class of ionic and electronic isotropic systems.[19,20] In Fig. 5 we show the dependence of the exponent s as a function of the concentration parameter p. In particular it is possible to see a decreasing behavior of s when p grows (for a fixed value of $w^{0\updownarrow}/w^{0\leftrightarrow}$). Therefore we obtain a frequency insensitivity of $\mathrm{Re}[D^{\updownarrow}(2\pi f)]$ when there are no vertical bonds broken. Besides, a similar type of behavior can also be observed if the analysis is modified considering s as a function of the rate $w^{0\updownarrow}/w^{0\leftrightarrow}$, with the bond concentration p remaining fixed. The imaginary part of $D^{\updownarrow}(2\pi f)$ is plotted in Fig. 4. In this plot it is possible to see a characteristic peak and the relaxation to zero for high frequencies. We also observe a linear dependence on $\mathrm{Im}[D^{\updownarrow}(2\pi f)]$ versus $2\pi f$ for low frequencies.

In the very high-frequency limit $2\pi f\rightarrow\infty$, performing a series expansions of the quantity $[G^0_{(1,0),(0,0)}(u)-G^0_{(0,0),(0,0)}(u)]$ appearing in Eq. (3.2), we obtain

$$D^{\updownarrow}(2\pi f)\simeq pw^{0\updownarrow}+i\frac{2p(1-p)(w^{0\updownarrow})^2}{2\pi f}. \tag{3.3}$$

Note that in this limit the behavior of the nonisotropic generalized diffusion constant is the same as the 1D unbiased case.[7] This fact can heuristically be understood because at short times ($u\rightarrow\infty$), the behavior of $D^{\updownarrow}(2\pi f)$ is mainly affected by the vertical bonds. The RW dispersion in the vertical direction mainly depends on $w^{\updownarrow}$ and not on the perpendicular hopping rate. The low-frequency behavior of $D^{\updownarrow}(2\pi f)$ is obtained performing a series expansion for $u\sim 0$ in Eq. (3.2), which then reads

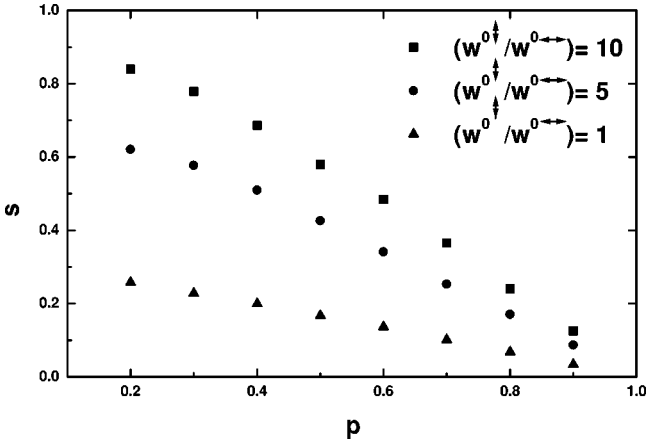

FIG. 5. Behavior of the exponent s in the power law $\sigma(2\pi f)\propto(2\pi f)^s$. This exponent is shown here as a function of concentration of the conducting bonds p in the vertical direction, for several values of the rate $w^{0\updownarrow}/w^{0\leftrightarrow}$.

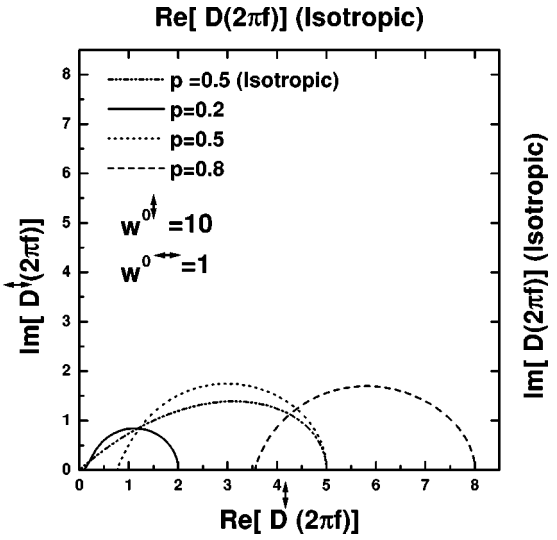

FIG. 6. The Cole-Cole diagram, $\mathrm{Im}[D^{\updownarrow}(2\pi f)]$ versus $\mathrm{Re}[D^{\updownarrow}(2\pi f)]$, for different values of the parameters $w^{0\updownarrow}$ and $w^{0\leftrightarrow}$. Observe the almost semicircular characteristic and the departure of this behavior for lower values of p. For comparison we have represented here the curve for the isotropic disordered case $[\Gamma(w^{\leftrightarrow})=\Omega(w^{\updownarrow})=p\,\delta(w-1)+(1-p)\,\delta(w)]$ at the percolation threshold $(p_{\mathrm{iso}}=1/2)$.

$$
\begin{aligned}
&p w^{0\updownarrow}-w^{\updownarrow}_{\mathrm{eff}}+[(w^{\updownarrow}_{\mathrm{eff}})^2-w^{\updownarrow}_{\mathrm{eff}}w^{0\updownarrow}]\\
&\times\left(\frac{2\arctan(\sqrt{w^{\updownarrow}_{\mathrm{eff}}/w^{0\leftrightarrow}})}{\pi w^{\updownarrow}_{\mathrm{eff}}}-\frac{\pi}{8}\,\frac{2\pi f}{\sqrt{w^{\updownarrow}_{\mathrm{eff}}w^{0\leftrightarrow}}}\right)\\
&+i[(w^{\updownarrow}_{\mathrm{eff}})^2-w^{\updownarrow}_{\mathrm{eff}}w^{0\updownarrow}]\frac{2\pi f}{4\sqrt{w^{\updownarrow}_{\mathrm{eff}}w^{0\leftrightarrow}}}\\
&\times\left[\ln(2\pi f)-\ln\left(\frac{64w^{\updownarrow}_{\mathrm{eff}}w^{0\leftrightarrow}}{w^{\updownarrow}_{\mathrm{eff}}+w^{0\leftrightarrow}}\right)\right]=0. \qquad (3.4)
\end{aligned}
$$

From this equation, clearly when $2\pi f\to 0$ the real part of $D^{\updownarrow}(2\pi f)$ saturates and its imaginary part goes to zero.

The overall frequency response can alternatively be represented by using a Cole-Cole diagram $\{\mathrm{Im}[D^{\updownarrow}(2\pi f)]$ versus $\mathrm{Re}[D^{\updownarrow}(2\pi f)]\}$ as shown in Fig. 6. In this figure we find *almost* semicircular shapes, characteristic of this type of diagrams. It is also possible to observe a little departure from the semicircular plot for lower values of p. We find that this departure is independent of the rate $w^{0\updownarrow}/w^{0\leftrightarrow}$, teaching us that this departure is mainly produced by the (disorder) parameter p. On the other hand, the larger the rate $w^{0\updownarrow}/w^{0\leftrightarrow}$ is, the larger the diameter of the semicircular Cole-Cole plot will be. This can also be seen by a swift inspection of the real part of $D^{\updownarrow}(2\pi f)$. To make a comparison of our nonisotropic cases with the well-known isotropic one, we have represented a curve for the last, at the percolation threshold $(p_{\mathrm{iso}}=1/2)$. It is important to note that as a consequence of the anisotropy, there is a shift on the left limit of any Cole-Cole curve (dc limit) toward greater value of the $\mathrm{Re}[D^{\updownarrow}(2\pi f)]$. However, the isotropic case always goes to zero for $p<p_{\mathrm{iso}}$.

The dc conductivity corresponds to the limit $u\to 0$ in Eq. (3.4). Thus we reobtain our previously reported result[16]

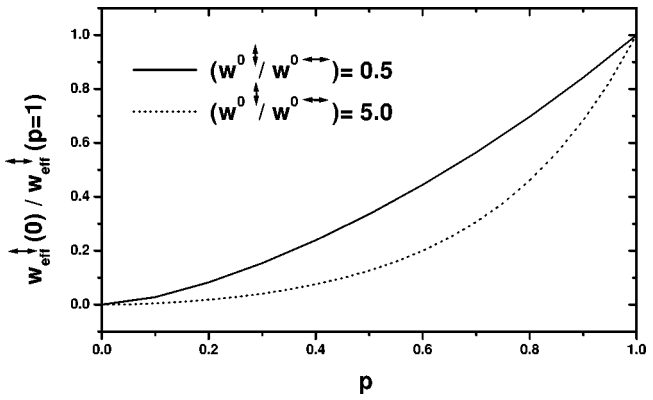

FIG. 7. dc conductivity from the nonisotropic EMA, Eq. (3.5), for two values of the rate $w^{0\updownarrow}/w^{0\leftrightarrow}$ as a function of the concentration p. Note that as consequence of anisotropy the *percolation threshold* is shifted to $p=0$.

$$
p w^{0\updownarrow}-w^{\updownarrow}_{\mathrm{eff}}(0)=\frac{2}{\pi}(w^{0\updownarrow}-w^{\updownarrow}_{\mathrm{eff}}(0))\arctan(\sqrt{w^{\updownarrow}_{\mathrm{eff}}(0)/w^{0\leftrightarrow}}). \qquad (3.5)
$$

This zero-frequency limit was also obtained by Bernasconi[14] by using Kirpatrick's approach. From Eq. (3.5) it is easy to see that for $p=0$ (all the bonds in the vertical direction are broken) the solution is $w^{\updownarrow}_{\mathrm{eff}}(0)=0$. In the opposite case $(p=1)$, the solution is $w^{\updownarrow}_{\mathrm{eff}}(0)=w^{0\updownarrow}$ as was expected. In Fig. 7 we have plotted the effective rate (electric conductivity in the vertical direction) using the rescaled quantities $\tilde{w}^{\updownarrow}_{\mathrm{eff}}(0)\equiv w^{\updownarrow}_{\mathrm{eff}}(0)/w^{\updownarrow}_{\mathrm{eff}}(p=1)$ and $\tilde{w}^{0}\equiv w^{0\updownarrow}/w^{0\leftrightarrow}$, as a function of the concentration p (for two values of $\tilde{w}^{0}$). A comparison with Monte Carlo simulations has been presented before.[16] At this point it is useful to note that anisotropic percolation models have broadly similar properties to those of isotropic networks. However, the critical concentration $p_c(=1/d)$ in the isotropic case becomes a ''critical surface'' in the nonisotropic model. This fact can also be seen from Eq. (3.5) because the threshold to zero conductivity $[\tilde{w}^{\updownarrow}_{\mathrm{eff}}(0)=0]$ is shifted to $p=0$. This phenomenon can also be heuristically interpreted because the walker can reach any place in the lattice. For any $p\neq 0$ there are always connecting paths between any two sites. We must note that our nonisotropic model reproduces the 1D and 2D dc isotropic result. Taking the limit $w^{0\leftrightarrow}\to 0$ in Eq. (2.9) we obtain for the effective rate $w^{\updownarrow}_{\mathrm{eff}}(0)=\langle 1/w^{\updownarrow}\rangle^{-1}$, that is, the 1D mean effective rate.[6] On the other hand, if in Eq. (2.9) we consider the limit $w^{0\leftrightarrow}\to w^{\updownarrow}_{\mathrm{eff}}(0)$, we obtain $\langle(w^{\updownarrow}_{\mathrm{eff}}(0)-w^{\updownarrow})/(w^{\updownarrow}_{\mathrm{eff}}(0)+w^{\updownarrow})\rangle=0$, that is, the self-consistent 2D equation for isotropic bond disordered models.[7]

B. Weak and strong disordered model

To consider other cases of disorder in our formalism, we introduce here a monoparametric distribution function:

$$
\Omega(w)=\begin{cases}(1-\alpha)w^{-\alpha}, & 0<w\leqslant 1\\ 0, & \text{otherwise},\end{cases} \qquad (3.6)
$$

which describes weak and strong disorder by changing the parameter α. If $-\infty<\alpha\leqslant 0$, we get a sort of *weak disorder*

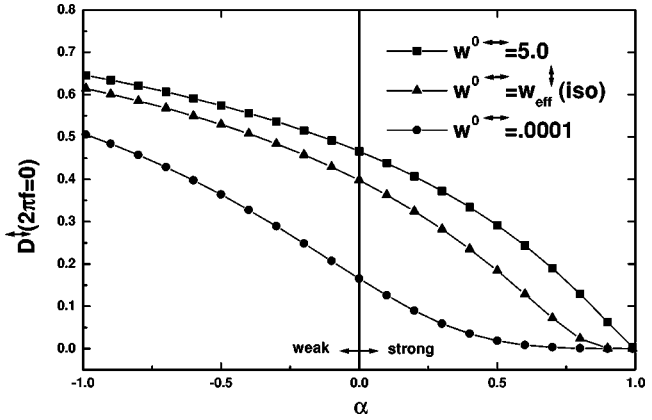

FIG. 8. dc diffusion coefficient in the vertical direction for different values of the parameter $w^{0\leftrightarrow}$, in presence of weak ($\alpha \leqslant 0$) and strong disorder ($0<\alpha<1$). Also, we have plotted the isotropic case (full triangles).

(only a finite number of inverse moments $\langle 1/w^k \rangle$, with $k=1,2,3,\ldots$, remain finite), whereas if $0<\alpha<1$ we get a class of *strong disorder* (all the inverse moments diverge). As we have pointed out before, in this work we will consider only the disorder in the vertical direction. In this section we will be interested in the dc limit of Eq. (2.9) and we will consider the disorder to be characterized by Eq. (3.6). The spectral study of $w^{\updownarrow}_{\rm eff}(u)$ for $u \neq 0$ can also be done in a similar way. Solving Eq. (2.9) by using $w^{\leftrightarrow}$ as nonrandom and Eq. (3.6) as the probability distribution for the random variable $w^{\updownarrow}$, the self-consistent condition reads

$$\frac{w^{\updownarrow}_{\rm eff}(0)}{1-\alpha}\,{}_2F_1[1,1-\alpha;2-\alpha;-\mathcal{F}(w^{\updownarrow}_{\rm eff}(0),w^{0\leftrightarrow})] - \frac{1}{2-\alpha}\,{}_2F_1[1,2-\alpha;3-\alpha;-\mathcal{F}(w^{\updownarrow}_{\rm eff}(0),w^{0\leftrightarrow})]=0. \tag{3.7}$$

Here, ${}_2F_1(a,b;c;Z)$ is the hypergeometric function, where the argument Z is given by the function

$$\mathcal{F}(w^{\updownarrow}_{\rm eff}(0),w^{0\leftrightarrow}) = 2\arctan\left(\sqrt{\frac{w^{\updownarrow}_{\rm eff}(0)}{w^{0\leftrightarrow}}}\right) \Bigg/ \left[\pi w^{\updownarrow}_{\rm eff}(0) - 2w^{\updownarrow}_{\rm eff}(0)\arctan\left(\sqrt{\frac{w^{\updownarrow}_{\rm eff}(0)}{w^{0\leftrightarrow}}}\right)\right]. \tag{3.8}$$

In Fig. 8 we show the behavior of the $w^{\updownarrow}_{\rm eff}(0)$ for $-1<\alpha<1$ and for different values of the parameter $w^{0\leftrightarrow}$. Also we show the isotropic coherent rate $w_{\rm eff}(0)$. Note that the isotropic case can also be obtained by taking the limits $w^{0\leftrightarrow} \to w^{\updownarrow}_{\rm eff}(0)$ and $w^{\updownarrow}_{\rm eff}(0) \to w_{\rm eff}(0)$ in our self-consistent Eq. (3.7). This is so because in this limit $\mathcal{F}(w^{\updownarrow}_{\rm eff}(0),w^{0\leftrightarrow}) \to 1/w_{\rm eff}(0)$.

Let us now comment about the behavior of the diffusion coefficient in the vertical direction. The lattice parameter has been taken $\Lambda=1$; thus the diffusion coefficient is equal to the coherent rate. For α in the range $[-1,0]$, the isotropic coherent rate is bounded by the values $0.397<w_{\rm eff}(0)<0.614$. Therefore we found that if $w^{0\leftrightarrow}$ is lower than the minimum value of $w_{\rm eff}(0)$, the behavior of the nonisotropic coherent rate $w^{\updownarrow}_{\rm eff}(0)$ is always lower than the isotropic one (in the same range of α). The opposite case is also valid. If $w^{0\leftrightarrow}$ is larger than the maximum value of $w_{\rm eff}(0)$ the behavior of the nonisotropic coherent rate $w^{\updownarrow}_{\rm eff}(0)$ is always larger than the isotropic one. For the strong disorder case $\alpha \in (0,1)$, a similar conclusion can also be seen from Fig. 8. The remarkable point is that for strong disorder the system can mimic a quasi-1D behavior. This fact is also seen from Fig. 8 for $\alpha \in (0,1)$. For the isotropic 2D *bond* disordered models the system has always a finite dc conductivity.[21] This is not the case in the isotropic *site* disordered α model, where in any dimension the dc conductivity goes to zero! Nevertheless, for the nonisotropic *bond* disordered α model and when $w^{0\leftrightarrow}/w_{\rm eff}(0) \ll 1$ the dc conductivity goes to zero, for $\alpha \in (0,1)$, very much before the isotropic case (see the full circles in Fig. 8). This fact can be interpreted as showing that the nonisotropic system has a quasi-1D behavior. In the opposite case when $w^{0\leftrightarrow}/w_{\rm eff}(0) \gg 1$ the transition to zero dc conductivity in the limit $\alpha \to 1$ is much more abrupt than in the isotropic case as can be expected from the high anisotropy. These behaviors can heuristically be understood: If the perpendicular rate is larger than the isotropic coherent rate, the effective conducting paths in the vertical direction are enhanced by the probable (large) excursions in the ordered direction [because $w^{0\leftrightarrow}>w_{\rm eff}(0)$]. Therefore the conductivity in the disordered direction is larger than the isotropic case. The opposite case $w^{0\leftrightarrow}<w_{\rm eff}(0)$ can also be understood by the same arguments, leading then to a reduction to the effective conducting paths in the vertical direction.

The frequency-dependent diffusion coefficient (for the α model of disorder) can also be obtained following the same methodology as for the dc conductivity. Now the self-consistent condition is the same as Eq. (3.7), but a new argument $\mathcal{F}(w^{\updownarrow}_{\rm eff},w^{0\leftrightarrow},u)$ in the hypergeometric function must be inserted (therefore involving elliptic integrals).

IV. CONCLUSIONS

The results presented here give insight into the frequency-dependent behavior of the conductivity in nonisotropic bond disordered models. We have worked out this problem in a generalized context of the well-known EMA. Our approach leads to a set of coupled self-consistent equations to be able to consider the anisotropy of the random media. Our approach is quite general and provides the possibility to study other models of disorder in two- or three-dimensional lattices. In the present work we have restricted the analysis to the square lattices. Therefore we have worked with a pair of coupled nonlinear self-consistent equations, one for each coherent rate, namely $w^{\updownarrow}_{\rm eff}(u)$ and $w^{\leftrightarrow}_{\rm eff}(u)$. We have exemplified our method by considering two models of disorder (but only) in the vertical direction. Specifically, the anisotropic bond percolation model given by Eq. (3.1), and the anisotropic α model given by Eq. (3.6). These models illustrate the main characteristics of the procedure and allow us to get a better understanding of the problem of the nonisotropic electric conductivity. Within the present formalism we have also reobtained the dc conductivity previously reported by

using Kirkpatrick's scheme.[14–16] The present approach also allows us to get the complete frequency response in a unified way. For the nonisotropic percolation model, the lack of the percolation threshold, in comparison with the isotropic case ($p_c=1/2$), can be seen from Fig. 7. The corresponding spectral analysis shows that the Cole-Cole diagrams, for the nonisotropic case, have a shift in the low-frequency limit, as can be seen in Fig. 6. For this model of disorder, the frequency dependence of $\mathrm{Re}[D^{\updownarrow}(2\pi f)]$ shows a power-law dielectric response $[\sigma^{\updownarrow}(2\pi f)\propto(2\pi f)^s]$ at intermediate frequencies. From Fig. 5 it is possible to see that the exponent s depends on the quantity $w^{0\updownarrow}/w^{0\leftrightarrow}$, the rate between the intrinsic conductivities corresponding to the disordered and ordered axis. Also, it depends on the concentration p. Thus we have found that the value of the exponent s strongly depends on the physical parameters of the nonisotropic model. In Sec. III B we have found a quasi-1D behavior for the α model in the strong disorder region. Finally the density of states for anisotropic ordered lattices was reported. Expressions for the limits corresponding to 2D isotropic lattices and the 1D case have explicitly been calculated in Appendix A.

The temperature dependence of the spectral properties can be introduced in our framework through the temperature dependence of rates $w^{\updownarrow}$ and $w^{\leftrightarrow}$. The present approach allows us to study the interplay between the temperature activated hopping and the nonisotropic disorder phases in a unified theory.

ACKNOWLEDGMENTS

This work has been partially supported by grants from CONICET (PIP No. 4948) and Secretaría de Investigación de la Universidad Nacional del Comahue.

APPENDIX A: NONISOTROPIC PROBLEM

The solution of the general biased homogeneous one step master equation

$$\partial_t P_{m,n}(t)=AP_{m,n-1}(t)+BP_{m,n+1}(t)+CP_{m-1,n}(t)+DP_{m+1,n}(t)-(A+B+C+D)P_{m,n}(t), \tag{A1}$$

corresponding to the RW operator given by Eq. (2.5), can be mapped on the unbiased case through the transformation

$$P_{m,n}(t)=Q_{m,n}(t)\left(\frac{A}{B}\right)^{n/2}\left(\frac{C}{D}\right)^{m/2}\exp[-(A+B+C+D-2\sqrt{AB}-2\sqrt{CD})t], \tag{A2}$$

where $Q_{m,n}(t)$ is the solution of the anisotropic (unbiased) master equation

$$\partial_t Q_{m,n}=X(Q_{m,n+1}+Q_{m,n-1}-2Q_{m,n})+Y(Q_{m+1,n}+Q_{m-1,n}-2Q_{m,n}). \tag{A3}$$

Here there are only two (different) hopping rates: $X\equiv\sqrt{AB}$ and $Y\equiv\sqrt{CD}$.

We are interested in the Green's function of Eq. (A3). Performing a Laplace and Fourier transform in Eq. (A3), the solution corresponding to the initial condition $Q_{m,n}(t=0)=\delta_{m,m_0}\delta_{n,n_0}$ can be written as

$$G^0_{(m,n),(m_0,n_0)}(u)=\frac{1}{4\pi^2}\int_{-\pi}^{\pi}dq_1\int_{-\pi}^{\pi}dq_2\times\frac{\exp\{i[(m-m_0)q_1+(n-n_0)q_2]\}}{u+2[X(1-\cos q_2)+Y(1-\cos q_1)]}. \tag{A4}$$

Integrating over q_1 we obtain

$$G^0_{(m,n),(m_0,n_0)}=\frac{1}{4\pi Y}\int_{-\pi}^{\pi}dq_2\frac{e^{i(n-n_0)q_2}\left[\Delta-\frac{X}{Y}\cos q_2-\sqrt{\left(\Delta-\frac{X}{Y}\cos q_2\right)^2-1}\right]^{m-m_0}}{\sqrt{\left(\Delta-\frac{X}{Y}\cos q_2\right)^2-1}}, \tag{A5}$$

where $\Delta=1+X/Y+u/2Y$. From Eq. (A5) and using the relation

$$\Pi(\rho,k)+\Pi\left(\frac{k^2}{\rho},k\right)-K(k)=\frac{\pi}{2}\sqrt{\frac{\rho}{(1+\rho)(k^2+\rho)}}, \tag{A6}$$

for $0<k<1$, between the the complete elliptical integrals of the first kind, $K(k)$, and the third kind, $\Pi(\rho,k)$, we have calculated the following elements of G^0:

$$G^0_{(0,0),(0,0)}(u)=\frac{1}{2\pi\sqrt{XY}}kK(k), \tag{A7}$$

where

$$k=\sqrt{\frac{16XY}{(u+4X)(u+4Y)}} \tag{A8}$$

and

$$G^0_{(1,0),(0,0)}(u)=\frac{1}{\pi\sqrt{XY}}k\left[\left(\frac{1}{2}+\frac{1}{\rho_1}\right)K(k)-\left(1+\frac{1}{\rho_1}\right)\Pi(\rho_1,k)\right], \quad \text{(A9)}$$

$$G^0_{(0,1),(0,0)}(u)=\frac{1}{\pi\sqrt{XY}}k\left[\left(\frac{1}{2}+\frac{1}{\rho_2}\right)K(k)-\left(1+\frac{1}{\rho_2}\right)\Pi(\rho_2,k)\right], \quad \text{(A10)}$$

where $\rho_1=4Y/(u+4X)$ and $\rho_2=4X/(u+4Y)$. The expressions (A9) and (A10) are symmetrical under the transformation $X\leftrightarrow Y$, as we can expect. Additionally, we note that the isotropic two-dimensional case is recovered with the identification $X=Y$. In this situation, Eq. (A7) results in

$$G^{0(\mathrm{iso})}_{(0,0),(0,0)}=\frac{1}{2\pi Y(1+u/4Y)}K\left(\frac{1}{(1+u/4Y)}\right), \quad \text{(A11)}$$

and Eqs. (A9) and (A10) coalesce in the expression

$$G^{0(\mathrm{iso})}_{(1,0),(0,0)}=\frac{1}{2\pi Y}K\left(\frac{1}{(1+u/4Y)}\right)-\frac{1}{4Y}. \quad \text{(A12)}$$

In the text we are concerned with unbiased systems: $X=A=B$ and $Y=C=D$.

Density of states

From Eq. (A4) the band of relaxation modes B results in $B=[-4(X+Y),0]$. The density of states (relaxation modes) per site is given by[6]

$$N(\lambda)=\mp\frac{1}{\pi}\lim_{\eta\to 0^+}\mathrm{Im}\,G^0_{(0,0),(0,0)}(\lambda\pm i\eta) \quad \text{(A13)}$$

for $\lambda\in B$. In the complex plane, the function $K(k)$ has branch cuts connecting $+1$ and $+\infty$ and -1 and $-\infty$, respectively, on the real axis. For $u<0$ we define

$$B_1=[-4(X+Y),-4W_>]\cup(-4W_<,0), \quad \text{(A14)}$$

$$B_2=(-4W_>,-4W_<),$$

$$B_3=(-\infty,-4W_>),$$

where $W_>=\max(X,Y)$ and $W_<=\min(X,Y)$. For $u>0$ or $u\in B_3$ we find $|k|<1$, but for $u\in B_1$ we get the condition $|k|>1$. We must note that for $u\in B_2$ result $k=i\tilde{k}$, where

$$\tilde{k}=\sqrt{-\frac{16XY}{(u+4X)(u+4Y)}}. \quad \text{(A15)}$$

For $u\in B_1$, taking $k=k_R+i\epsilon$, $\epsilon\sim 0^+$, and using the known expressions[22]

$$K(k)=k^{-1}[K(k^{-1})+iK(k^{-1}\sqrt{k^2-1})] \quad (\text{for } k_R>1), \quad \text{(A16a)}$$

$$K(k)=|k|^{-1}[K(k^{-1})-iK(k^{-1}\sqrt{k^2-1})] \quad (\text{for } k_R<-1), \quad \text{(A16b)}$$

we obtain for the anisotropic case

$$N(\lambda)=\frac{1}{2\pi^2\sqrt{XY}}K\left(\sqrt{-\frac{\lambda^2+4(X+Y)\lambda}{16XY}}\right). \quad \text{(A17)}$$

The elliptic integral $K(k)$ behaves as $\ln[4/\sqrt{1-k^2}]$ as $k\to 1$. Thus $N(\lambda)$ has logarithmic singularities at the inner edges ($-4W_>$ and $-4W_<$), and exhibits at both external band edges $[-4(X+Y)$ and $0]$ a discontinuity.

For $u\in B_2$, using the expresions[22]

$$K(i\tilde{k})=\frac{1}{\sqrt{1+\tilde{k}^2}}K\left(\sqrt{\frac{\tilde{k}^2}{1+\tilde{k}^2}}\right) \quad \text{(A18)}$$

and

$$\bar{k}=\sqrt{\frac{\tilde{k}^2}{1+\tilde{k}^2}}=\sqrt{-\frac{16XY}{u^2+4(X+Y)u}}<1, \quad \text{(A19)}$$

we obtain

$$G_{(0,0),(0,0)}(u)=\frac{i}{2\pi\sqrt{XY}}\bar{k}K(\bar{k}). \quad \text{(A20)}$$

Hence we find

$$N(\lambda)=\frac{2}{\pi^2}\frac{1}{\sqrt{-(\lambda^2+4(X+Y)\lambda)}}\times K\left(\sqrt{-\frac{16XY}{\lambda^2+4(X+Y)\lambda}}\right). \quad \text{(A21)}$$

$N(\lambda)$ also has logarithmic singularities at the edges of B_2 ($-4W_>$ and $-4W_<$).

We note that the isotropic two-dimensional case is recovered with the identification $X=Y$. The band of relaxation modes becomes the interval $(-8Y,0)$ and B_2 disappears. However, the density of states retains a logarithmic singularity at the center of the band. Additionally, the one-dimensional case is recovered taking $W_<=0$. The band becomes the interval $(-4W_>,0)$ and B_1 disappears. Since $K(0)=\pi/2$ we obtain the expresion $N(\lambda)=1/\pi\sqrt{-\lambda(\lambda+4W_>)}$ from Eq. (A21). In this case, the density of states presents a power-law divergent behavior at the band edges.

Taking the substitution $\lambda=-\omega^2$, the problem is mapped on the frequency spectrum of oscillations in 2D anisotropic lattices whose vibrations are transverse (normal to the equilibrium plane of the lattice).

APPENDIX B: SINGLE IMPURITY PROBLEM

The perturbed problem is defined by $H_i=H_0+V$, where the H_0 and V are given by Eqs. (2.5) and (2.6). The corresponding Green's function $G^i=(u-H_i)^{-1}$ can be written in terms of the Green's function associated to the homogeneous lattice, $G^0(u)=(u-H_0)^{-1}$. This can be performed in

d-dimensional hypercubic lattices for any selected direction of the impure bond. Defining $V^1=|a\rangle b_1\langle a|$, $H_1=H_i-V^1$, $G^1=(u-H_1)^{-1}$, and performing a Dyson expansion

$$G^i=G^1+G^1V^1G^1+G^1V^1G^1V^1G^1+\cdots, \tag{B1}$$

we can express G^i in terms of G^1:

$$G^i_{\alpha\beta}=G^1_{\alpha\beta}+G^1_{\alpha a}b_1G^1_{a\beta}(1-b_1G^1_{aa})^{-1}. \tag{B2}$$

The same scheme must be applied defining $V^2=|a\rangle b_2\langle b|$, $H_2=H_1-V^2$, and $G^2=(u-H_2)^{-1}$. This enables us to express G^1 in terms of G^2:

$$G^1_{\alpha\beta}=G^2_{\alpha\beta}+G^2_{\alpha a}b_2G^2_{b\beta}(1-b_2G^2_{ba})^{-1}. \tag{B3}$$

Then, defining $V^3=|b\rangle b_3\langle a|$, $H_3=H_2-V^3$, and $G^3=(u-H_3)^{-1}$, we can express G^2 in terms of G^3:

$$G^2_{\alpha\beta}=G^3_{\alpha\beta}+G^3_{\alpha b}b_3G^3_{a\beta}(1-b_3G^3_{ab})^{-1}. \tag{B4}$$

Finally, defining $V^4=|b\rangle b_4\langle b|$, we obtain $H_0=H_3-V^4$ and we can express G^3 in terms of G^0, the homogeneous Green's function:

$$G^3_{\alpha\beta}=G^0_{\alpha\beta}+G^0_{\alpha b}b_4G^0_{b\beta}(1-b_4G^0_{bb})^{-1}. \tag{B5}$$

Note that by definition $b_3=-b_1$, $b_2=-b_4$. Inverting the process, we finally obtain the exact expression

$$G^i_{ab}=\frac{G^0_{ab}+b_4(G^0_{ab}G^0_{ba}-G^0_{aa}G^0_{bb})}{1+b_1(G^0_{ab}-G^0_{aa})+b_4(G^0_{ba}-G^0_{bb})}. \tag{B6}$$

The inhomogeneous Green's function appearing in Eq. (2.7) is calculated in absence of bias; i.e., $A=B$ and $C=D$. Thus results $W_{ab}=W_{ba}$ and $b_1=b_4$. Given the homogeneity of the unperturbed lattice we always have $G^0_{aa}=G^0_{(0,0),(0,0)}$ for any site a and as consequence of the no bias assumed, results $G^0_{ab}=G^0_{ba}$ for any pair of nearest-neighbor sites a, b. In the text we have chosen the site $b=(0,0)$ and the two possibilities (1,0) and (0,1) for the site a.

*Senior Independent Research Associate at Consejo Nacional de Investigaciones Científicas y Tecnológicas (CONICET). Electronic address: caceres@cab.cnea.gov.ar

[1] C.R. Berg, Geophysics **60**, 1070 (1995).
[2] One of the main problems to model the electrical conductivity in these systems arises from strong anisotropy of porous reservoir rocks, which can be produced by geometrical or intrinsic conductivity factors (Ref. 3).
[3] J.M.V.A. Koelman and A. de Kuijper, Physica A **247**, 10 (1997).
[4] H. Jhans, D. Kim, R.J. Rasmussen, and J.M. Honig, Phys. Rev. B **54**, 11 224 (1996).
[5] H. Scher and M. Lax, Phys. Rev. B **7**, 4491 (1973).
[6] S. Alexander, J. Bernasconi, W.R. Schneider, and R. Orbach, Rev. Mod. Phys. **53**, 175 (1981).
[7] T. Odagaki and M. Lax, Phys. Rev. B **24**, 5284 (1981).
[8] E. Hernández-García, M.A. Rodríguez, and M. San Miguel, Phys. Rev. B **42**, 10 653 (1990).
[9] P.A. Pury and M.O. Cáceres, Phys. Rev. B **55**, 3841 (1997).
[10] E. Hernández-García, M.O. Cáceres, and M. San Miguel, Phys. Rev. A **41**, 4562 (1990); E. Hernández-García and M.O. Cáceres, *ibid.* **42**, 4503 (1990).
[11] P.A. Pury, M.O. Cáceres, and E. Hernández-García, Phys. Rev. E **49**, R967 (1994).
[12] M.O. Cáceres, H. Matsuda, T. Odagaki, D.P. Prato, and W. Lamberti, Phys. Rev. B **56**, 5897 (1997).
[13] T. Odagaki, M. Kawasaki, M.O. Cáceres, and H. Matsuda, in *Statistical Physics: Experiments, Theory and Computer Simulations*, edited by M. Tokuyama and I. Oppenheim (World Scientific, Singapore, 1997), p. 171.
[14] J. Bernasconi, Phys. Rev. B **9**, 4575 (1974).
[15] P.G. Toledo, H. Ted Davis, and L.E. Scriven, Chem. Eng. Sci. **47**, 391 (1992).
[16] E.R. Reyes, M.O. Cáceres, and P.A. Pury, Physica A **258**, 1 (1998).
[17] J.W. Haus and K.W. Kehr, Phys. Rep. **150**, 263 (1987); G.H. Weiss, *Aspects and Applications of the Random Walk* (North-Holland, Amsterdam, 1994); N.G. van Kampen, *Stochastic Processes in Physics and Chemistry*, 2nd edition (North-Holland, Amsterdam, 1992).
[18] A. Compte and M.O. Cáceres, Phys. Rev. Lett. **81**, 3140 (1998).
[19] K. Funke, Z. Phys. Chem., Neue Folge **154**, 251 (1987).
[20] M.O. Cáceres and E.R. Reyes, Physica A **227**, 277 (1996).
[21] S. Alexander, Phys. Rev. B **23**, 2951 (1981).
[22] T. Morita and T. Horiguchi, J. Math. Phys. **12**, 981 (1971).